ADVANCES IN PHYSICS, 1983, VOL. 32, NO. 3, 361–452

Electronic structure of amorphous semiconductors

By JOHN ROBERTSON
Central Electricity Research Laboratories, Leatherhead, Surrey, England

[Received 26 May 1983]

ABSTRACT

We review the bonding in a wide range of non-crystalline materials, such as the elemental and compound amorphous semiconductors, liquid semiconductors and, briefly, some oxide glasses and amorphous silicon dioxide. The review concentrates on the experimental determination of electronic structure from photoemission, optical spectra and core spectra and on its theoretical description, particularly using tight-binding methods. The review also describes the bonding at defects in amorphous semiconductors and in particular that of dopants and hydrogen in hydrogenated amorphous silicon (a-Si : H).

CONTENTS

§1. Introduction

A variety of important materials do not possess the periodic long-range order of crystals—liquids, amorphous solids and glasses. In many cases their electronic structures are similar to those of their respective crystals, because the atoms have retained a similar nearest-neighbour environment or short-range order (SRO), or bonding [1, 2]. In this review, we concentrate on amorphous semiconductors, whose bonding is predominantly covalent.

Electronic structure calculations of crystals use highly developed methods such as pseudopotentials, orthogonalized plane waves or muffin tin potentials. However, their ease of use requires the presence of periodicity and the validity of Bloch's theorem. When the wave-vector **k** is no longer a good quantum number approaches depending only on SRO, such as atomic orbital methods and tight-binding, become more useful.

The interest in amorphous semiconductors coincided with the development of photoemission techniques to measure the valence band density of states [3, 4]. It was quickly appreciated that even model calculations using highly simplified tight-binding methods were valuable for comparing the bonding and density of state spectra of crystalline and amorphous semiconductors. These tight-binding (TB) techniques have since been refined by calibrating on photoemission spectra and more accurate crystal calculations, so we can now confidently describe the electronic states of the valence and lower conduction bands of semiconductors in a TB scheme, often using only interactions between nearest-neighbour atomic orbitals.

The covalent bonding of amorphous semiconductors usually produces co-ordinations in which each atom satisfies its local valence requirements. This results in the '8-N' or octet rule, linking co-ordination N_c to atomic valence N as $N_c = 8 - N$ for $N \geqslant 4$ but $N_c = N$ for $N < 4$. This rule is the origin of many bonding similarities and is easily understood from a tight-binding viewpoint.

The review begins with a discussion of methods for calculating electronic structure, emphasizing the TB [5, 6] and pseudopotential [7, 8] methods. We pay attention to giving the reader qualitative insight using the simplest TB methods and also to developing a quantitative method for later use. The elemental amorphous semiconductors are first discussed in some detail, followed by the alloys and compounds. Localized states and mobility edges are a distinctive feature of disordered semiconductors [1]. We discuss localized states which relate to changes in SRO but omit the formal theory of localization and the metal/non-metal transition (MNMT). Thus we pay special attention to compositional-dependent MNMTs [9–11] and to localized states due to abnormal bonding configurations such as defects and impurities [12–16]. The study of electronic structure presupposes a knowledge of the atomic structure. While this is usually taken for granted for crystals, its determination for non-crystalline systems is frequently an arduous task. Most of the necessary information is usually extracted from diffraction studies, but in polyatomic systems the task quickly increases in complexity to the extent that even the type of nearest neighbour may not be known. Thus we preface each section with a review of how the local atomic order was determined [17–23]. It is now appreciated that many electronic properties of amorphous semiconductors are controlled by their defects and impurities [12–16, 24–26], as are crystals. The ability to dope hydrogenated amorphous silicon (a-Si : H) has led to the intense study of this system. Thus we review amorphous silicon (a-Si) in two stages, first the pure form a-Si in § 5 and then the hydrogenated and doped forms in § 8. We note in passing that the local structure of defects and dopant sites is frequently not known experimentally but must be inferred by applying bonding rules. This illustrates both the need for and the successes of our present understanding of electronic structure and bonding.

§ 2. Calculation methods

2.1. *The problem: SRO in a-Ge, an introductory example*

In order to appreciate the various methods and approximations used to calculate electronic structure, we first describe the short-range order of a typical amorphous semiconductor: a-Ge. Most of the experimentally accessible information on SRO in a non-crystalline system is contained in the radial distribution function, $J(r)$ or rdf [17, 27–30]. This is defined as the atomic probability density at a distance r from a reference atom. The loss of long-range order (LRO) in a-Ge is visible in that the rdf tends to a uniform distribution, $J(r)=4\pi r^2\rho_0$ at large distances, but the sharpness of the early peaks shows the preservation of SRO (fig. 1). The first peak due to nearest neighbours occurs at $r_1=2{\cdot}45$ Å and its area corresponds to four atoms†, as for crystalline (c-)Ge. The peak is very sharp with little more than thermal broadening in a-Ge, as in most glasses or well-annealed amorphous semiconductors. The bond angle θ is found from the second peak at r_2 by $r_2=2r_1\cos(\theta/2)$. Its average value of $109{\cdot}5°$ is that expected for tetrahedral sp^3 bonding. The larger width of the second peak reflects bond angle deviations of $\pm 9°$. Since this peak is incompletely separated from subsequent peaks, the second neighbour spectrum is found by folding over the

† In fact the first peak contains less than four atoms, which may be related to the large number of defects and reconstructions in a-Ge, discussed in § 7.4.

Fig. 1

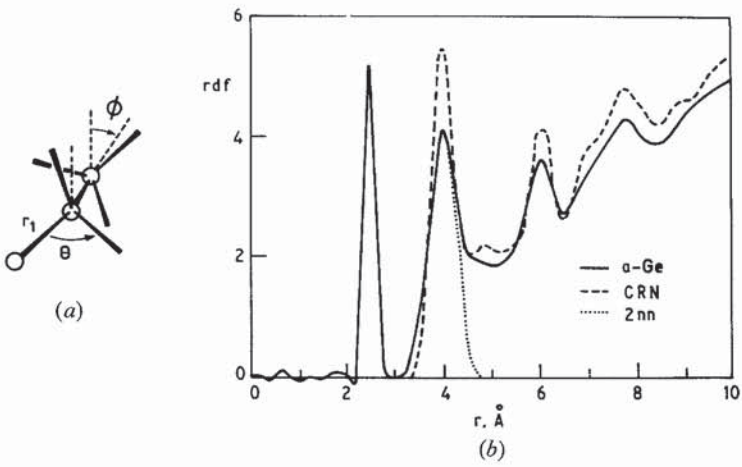

(*a*) Definition of the dihedral angle ϕ in Ge. (*b*) The rdf of a-Ge.

leading edge. The third neighbour peak contains information on the dihedral angle distribution, but generally a model is needed to partition $J(r)$ into higher order correlations.

Continuous random networks (CRN) were developed to model covalent network glasses like a-SiO_2 or a-Ge [29–36]. The networks are constructed by representing atoms and bonds by balls and sticks and connecting them together randomly without loose ends or 'dangling bonds' [31]. Topological disorder now appears because the sites of a-Ge need no longer be connected by sixfold rings of bonds. Networks can be constructed for a-Ge without further specification. Minimum non-bonded distances must also be given for elements with lower co-ordinations like As or Se [37–39]. In multicomponent systems the degree of chemical ordering (the proportion of unlike atom bonding) must be specified. The experimental rdf and the building criteria of CRNs are related to the bonding rules of amorphous systems. It is found that the first neighbour co-ordination number (N_c), r_1 and θ are very similar to those of some crystalline polytype, even for an alloy. The bond length r_1 is particularly well defined [21].

CRNs are now appreciated to be idealized models of the structure of amorphous semiconductors and glasses. They do not describe possible clustering effects or intermediate-range order on the 10–30 Å scale [19, 20]. We see later how such order is related in recent theories to the number of defects, and in binary glasses to the degree of chemical order [40].

2.2. *The tight-binding method (TB)*

The total hamiltonian contains three types of interactions, those between nuclei, between electrons and nuclei, and between electrons. Anticipating the discussion of pseudopotentials, the core electrons can be combined with the nuclei as 'cores' giving a valence electron hamiltonian of the form:

$$H = H_{cc} + H_{ce} + H_{ee}, \tag{1}$$

where c = core and e = valence electrons.

The simplest electronic hamiltonian is given by the Hartree approximation in which each electron is taken to move in a 1-electron potential, the effective potential of the stationary cores and the other valence electrons, reducing H to an effective H_{ce}. The tight-binding and many pseudopotential methods correspond to this limit.

The tight-binding (TB) method is a simplification of the linear combination of atomic orbitals (LCAO) method. The wavefunctions in LCAO are constructed as linear combinations of atomic or other localized orbitals $|i\rangle$ as:

$$m\rangle = \sum c_i |i\rangle$$

and the hamiltonian H_{ce} is expressed in terms of the orbitals $|i\rangle$. TB consists of retaining only selected one- and two-centred interactions, the hopping interaction $H_{ij} = \langle i|H|j\rangle$ and the overlap integral $S_{ij} = \langle i|j\rangle$. The energies or eigenvalues (E) are then found by solving the secular determinant:

$$\det|H_{ij} - ES_{ij}| = 0. \tag{2}$$

The TB method has had much success in molecules. It is frequently criticized in solid state applications because the $|i\rangle$ are insufficiently localized, producing poor conduction bands and requiring the retention of distant H_{ij}. However, the desire to investigate periodic systems has forced us to persevere and develop a quantitative TB scheme.

The standard form of tight-binding for semiconductors consists of three approximations. We take a basis set of four valence orbitals, one s and three p, we neglect the overlap of different orbitals $S_{ij} = \delta_{ij}$ and we retain only short-ranged interactions H_{ij}, often only those between nearest neighbours. Chemical pseudopotential theory [6, 41–44] provides a formal justification for many of these simplifications. The chemical pseudopotential method is one of a class of local orbital theories [45] in which an effective hamiltonian is derived: $H' = S^{-1}H$. H' is found to be shorter ranged than H itself and provides some justification for the neglect of more distant interactions. Also, the secular determinant obeyed by H' is the same form as that of H when overlap is neglected:

$$\det|H'_{ij} - E| = 0. \tag{3}$$

This provides a rationalization for the very popular approximation of neglecting overlap. A third question concerns the size of the TB basis set. Many workers worry about the effects of higher orbitals, particularly d orbitals. Louie [46] has recently shown that orthogonality constraints tend to repel such excited orbitals to higher energies, reducing their effects. This repulsion is particularly important in higher co-ordinations, but less important in molecules.

There are two philosophies for finding the interactions H_{ij}, either by explicit calculation or by treating them as disposable parameters and fitting to established energy spectra. Whichever method is chosen it is desirable that the H_{ij} retain a 'physical significance', being relatively environment-independent and transferable.

We mention three means of calculating TB interactions, the fitting method is described shortly:

(1) Extended Huckel Theory (EHT) [47] retains the overlap integrals and uses the secular equation (2). It parametrizes H_{ij} against S_{ij} according to relations such as:

$$H_{ij} = \tfrac{1}{2} K S_{ij}(H_{ii} + H_{jj}), \tag{4}$$

with K a constant of order 1·5. EHT is a quick method favoured for molecules and in early solid-state calculations. Its two major problems are that K is often different for s or p orbitals, causing inverted band orderings when chosen incorrectly [48]. EHT also overestimates distant interactions because H_{ij} decays more quickly than S_{ij} itself.

(2) The overlap reduction method calculates H_{ij} and S_{ij} and then reduces S_{ij} by empirical factors [49, 50].

(3) Chemical pseudopotential theory itself gives the simplest and most reliable prescription for calculating H_{ij} using the so-called 'Wigner trick potential' [6].

2.3. *The empirical pseudopotential method (EPM)*

EPM [5] is representative of the k-space calculations. It also has a Hartree hamiltonian operator:

$$H = -\frac{h^2}{2m}\nabla^2 + V_p(r), \tag{5}$$

where $V_p(r)$ is the effective one-electron potential acting on a valence electron. This screened potential transfers quite accurately between different environments, after normalization for any volume changes. The hamiltonian is solved using a basis of plane waves, the $|k\rangle$ of interest and those in nearby zones $|k+Q\rangle$. This gives the secular determinant:

$$\det\left|\frac{\hbar^2(k+Q)^2}{2m} - E - V_{Q,Q'}\right| = 0. \tag{6}$$

If $V_{Q,Q'}$ is only allowed to depend on $q = Q - Q'$, it is called a local potential. $V(q)$ is so strongly damped that in simple structures its value need only be specified at a few wave-vectors. For the diamond lattice of Si or Ge, only the three coefficients $V(111)$, $V(220)$ and $V(311)$ are taken to be non-zero [51]. Their values are found by fitting to experimental data such as optical reflectivity or angle resolved photoemision spectra (ARPES). For compounds the total pseudopotential is the product of atomic structure factors and form factors:

$$V(q) = \sum_i S_i(q) V_i(q), \qquad S(q) = \sum_{\text{sites}} e_j^{i\mathbf{q}\cdot\mathbf{r}_j}. \tag{7}$$

For complex crystal lattices $V_i(q)$ is required at many q values so it is often expressed in algebraic form but again only about four parameters per atom need fitting empirically [52].

The local EPM provides quantitative descriptions of the band structures of sp-bonded semiconductors and metals and also of the properties of sp metals related to their total energy such as phonon spectra and lattice stabilities [7, 53]. Non-local (angular-momentum and energy-dependent) corrections improve the agreement for states away from the gap [54]. However, all fixed-screening theories are unsuitable for situations where the electron density changes rapidly such as at surfaces or vacancies [55], or for total energy calculations of semiconductors.

2.4. *Atomic pseudopotentials*

The pseudopotentials considered so far have been the one-electron or screened potentials, equal to the bare core potential screened by the other valence electrons.

Atomic pseudopotentials have been developed in parallel with screened pseudopotentials, whether for solid-state applications [55, 56] or as model potentials for atomic and molecular applications [57, 58]. Recently, self-consistently screened atomic pseudopotentials have been developed to the stage where they are able to reproduce most total energy properties of semiconductors [59], whether of the bulk or for their co-ordination defects such as surfaces or vacancies. The valence electron hamiltonian is now:

$$H = T + H_v + H_\rho + H_{\text{exc}}, \tag{8}$$

with T the kinetic energy, H_v the atomic pseudopotential, H_ρ the self-consistent Coulombic potential of the valence electrons and H_{exc} the exchange-correlation energy. H_{exc} is usually calculated as a function of the local electron density, using the local density formalism (LDF) [8].

The LDF screening is local in real space, like Thomas–Fermi screening. Thus, screened atomic pseudopotentials can be used with either plane waves or localized basis orbitals such as gaussians. They were introduced to overcome the practical restriction of EPM to periodic, fully bonded systems and can in principle be used for random networks.

Early work on pseudopotentials emphasized the small size of H_v within the core radius due to cancellation, and constructed H_v to minimize its scattering and produce the smoothest pseudowavefuntion [60]. These are now termed the 'soft-core' pseudopotentials. Recently, the importance of 'norm-conserving' pseudopotentials was realized [61] in which the pseudowavefunction is defined to equal the true wavefunction outside the core radius. Such pseudopotentials also have the property of minimum energy dependence and maximum transferability between different bonding environment [8]. They are not, however, the weakest scatterers, and so belong to the class of 'hard-core' pseudopotentials.

LDF screened, norm-conserving pseudopotential calculations are now able to reproduce with high accuracy valence band energies [8, 62, 63], valence charge densities and various functions of the total energy such as phonon frequencies and lattice stabilities [62, 64], for semiconductors as well as metals. Their implementation requires more computer power than EPM because of the larger basis resulting from the stronger scattering, and it is computer power which ultimately limits their use for surfaces, defects and random networks.

There are two problems with LDF band structures. The LDF applies formally only to the ground state, or valence bands. Also the various approximate forms of the LDF used do not always handle properly the short wavelength screening introduced by hard-core potentials, causing an underestimation of band gaps, a well-known error of LDF bands. For example, a gap of around 0·6 eV is calculated for c-Si [8, 62, 63], compared to 1·1 eV experimentally. However, energy separations within the conduction bands are generally given correctly. Thus, until the LDF is improved for excited states we possess two types of pseudopotential results, the older empirical type with good valence and conduction bands [54], and the newer type with excellent valence bands and total energies but underestimated band gaps [8, 62].

2.5. *Dealing with disordered hamiltonians*

Calculations on disordered systems naturally require us to handle large hamiltonian matrices. In disordered magnetic systems a periodic lattice usually

remains and disorder appears in the site-to-site interactions. In amorphous semiconductors disorder is fundamentally topological, while the interactions themselves remain constant. Five general approaches can be identified.

The recursion [65] and equation of motion methods [66] each give the local density of states at specified sites in systems described by large hamiltonians. The recursion method recognizes that the local DOS depends largely on close interactions and is suited to the TB method. It reduces a hamiltonian of a three-dimensional network to that of a linear chain, which is then handled algebraically. The local DOS is found for the first site of this chain. The interactions down the chain tend to stabilize and, in practice, are truncated after a certain number of levels, dictated by the bandwidth, the cluster size and the desired accuracy. Tested black-box routines for this method are available [65].

The equation of motion method [66] is frequently used for magnetic disorder and phonon studies but is easily adapted for use with TB hamiltonians. The local DOS is found by calculating the time-evolution of an initial state, as this provides a weighted sample of all eigenfunctions.

Often, when we desire to contrast various SROs it is better to create a set of lattices simulating the SROs than to compare particular sites in random networks. EPM can be used if the lattices are periodic and small enough. The calculations on crystalline Si polytypes are the best known example of this [67, 68].

Designing networks, polytypes or any structure specified in space often runs into the problem that some types of SRO are inconsistent with maintaining a fully connected network. An advantage of TB is that the external reference axes can be replaced by local, rotatable axes defined at each atom. The sites need no longer be located in real space and could actually lie over each other. Bethe lattice methods exploit this advantage [69–71]. Bethe lattices are singly corrected structures in which each vertex has the required co-ordination but there are no closed rings. The absence of closed rings allows a tractable solution, but also produces an unphysical retreat of some band edges. Cluster-Bethe lattice methods limit this fault and are widely used.

Finally, dilute disorder can be treated as a series of defects and studied by Green's function techniques [72].

§ 3. General applications

3.1. *The tight-binding view of bonding*

This section compares the tight-binding and pseudopotential descriptions of the covalent bond and the origin of band gaps. Although apparently different, the two theories provide surprisingly complementary views of covalence [5, 73]. The TB view also produces some valuable bonding rules such as the 8-N rule and the sizes of covalent bond angles. Two important simplified TB hamiltonians are discussed in some detail, the Weaire–Thorpe (WT) [74, 75] hamiltonian and the bond orbital model (BOM) [76, 77].

Bonds can be produced by the interactions of atomic orbitals or hybrid orbitals from two atoms. Hybrid orbitals are linear combinations of the atomic orbitals of a single atom which are now directional, thus producing a stronger bond than a pure atomic orbital [78]. In the systems considered here the covalent co-ordination never exceeds four, indicating that only s and p orbitals are primarily responsible for bonding. Generally, in amorphous semiconductors higher d orbitals have a marginal

effect on valence states and no valence shell expansion occurs, in contrast to the situation in molecules such as SF_6.

We noted that co-ordinations of many amorphous semiconductors obey the 8-N rule. This rule arises from the maximization of the bonding energy for a given number of valence electrons. Consider two hybrids on adjacent atoms directed towards each other, $|i\rangle$ and $|j\rangle$, of energy E_0 and their bonding interaction $V_2=\langle i|H|j\rangle$. The interaction V_2 produces a symmetric, bonding (σ) state at a lower energy, E_0+V_2 and an antisymmetric or antibonding (σ^*) state at E_0-V_2 (fig. 2). Each atom contributes one electron to this electron-pair bond, and these enter the σ state. Clearly, bonding energy is maximized by fully occupying σ states and leaving all σ^* states empty. A particular orbital can only form a bond if it is singly occupied before bonding occurs. Clearly empty or doubly occupied orbitals cannot bond. An atom with N valence electrons, with $N\leqslant 4$, can place each electron in separate orbitals and thus form N bonds, giving $N_c=N$. This leaves 4-N non-bonding unoccupied orbitals. If $N>4$ 8-N orbitals are singly occupied and form bonds leaving N-4 doubly occupied. The doubly occupied orbitals must remain non-bonding so only 8-N bonds can be formed, $N_c=8-N$.

Bond angles are largely determined by hybridization [78, 79]. We consider two hybrids whose fractional s content or hybridization is α^2. The first is:

$$|1\rangle=\alpha|s\rangle+(1-\alpha^2)^{1/2}|p_x\rangle. \tag{9}$$

The second must be orthogonal to $|1\rangle$. One possibility is:

$$|2\rangle=\alpha|s\rangle-\alpha(1-\alpha^2)^{-1/2}|p_x\rangle+(1-\alpha^2)^{1/2}|p_y\rangle. \tag{10}$$

These subtend an angle θ, related to the hybridization α^2 by:

$$\theta=\cos^{-1}\{-\alpha^2/(1-\alpha^2)\}. \tag{11}$$

This gives the tetrahedral bond angle, $\theta=109{\cdot}5^\circ$ for sp^3 hybrids. When $N<4$ the hybrids which form bonds are generally different from those which remain non-bonding. For such lower co-ordinations (e.g. H_2O, Se) the hybridization can be overestimated from the bond angle. One may think of this as the bonds no longer lying along the hybrid directions.

We now give an idealized description of the variation of co-ordinations and bond angles across the Periodic Table as an illustration of these rules (fig. 3). The alkali

Fig. 2

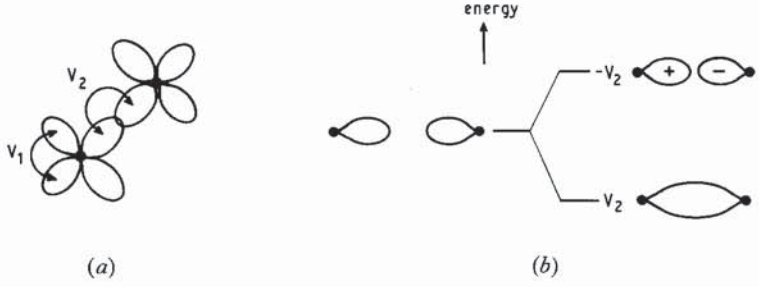

(*a*) Definition of the Weaire–Thorpe interactions V_1 and V_2. (*b*) Formation of σ and σ^* states from two orbitals.

Fig. 3

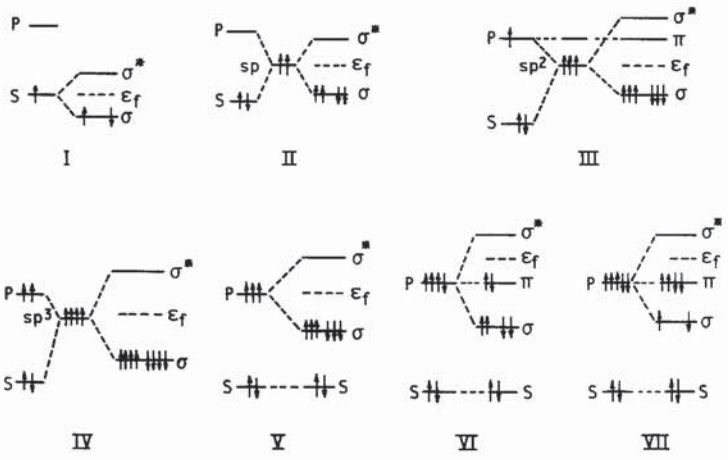

Bonding configurations of elements of groups I–VII.

elements of group I form single bonds and diatomic molecules with their s orbitals, e.g. gaseous Na_2. Alkaline earths might be expected to form two bonds. Group III elements such as B form three bonds using sp^2 hybrids, directed at 120° to each other within one plane. The non-bonding orbital is an unoccupied p_z orbital normal to this plane. Group IV elements form the canonical sp^3 hybrids and four bonds at 109·5° to each other. The group V elements form three bonds using their p orbitals. There is a small s hybridization which opens the bond angle above 90°. The non-bonding orbital is occupied and essentially s-like. The group VI elements form two p-like bonds. There is one s-like and one p-like non-bonding occupied orbital. The p-like state is referred to as a lone-pair or p_π state and has important consequences for the behaviour of these elements. The Fermi level lies in the gap between this occupied $p\pi$ orbital and the unoccupied σ^* orbital. The group VII elements are monovalent using their one singly occupied p orbital and the group VIII elements inert. This systematization of bond angles is referred to as Walsh's rules when applied to AX_n molecules [80].

3.2. *The Weaire–Thorpe hamiltonian*

The Weaire–Thorpe (WT) hamiltonian [74] was developed to study the topological behaviour of electron states and used to show that the covalent gap is not destroyed by disorder. The hamiltonian describes many bonding effects in an extremely simplified fashion. It uses a basis of sp^3 hybrids, retaining only the bonding interaction V_2 and the interaction between two hybrids on the same atom, $V_1 = \langle i|H|i'\rangle$. Its importance is that the band energies and the density of states can be found analytically for the diamond lattice and some disordered lattices. The basis has eight orbitals, four hybrids per site and two sites per lattice point, giving eight bands. Semiconducting bands are found if $V_2 > 2V_1$ (fig. 4). The band limits in the diamond structure are $V_2 - V_1$, $V_2 + 3V_1$ (valence band) and $-V_2 - V_1$, $-V_2 + 3V_1$ (conduction band). Topological disorder cannot create states outside these bounds, so the

Fig. 4

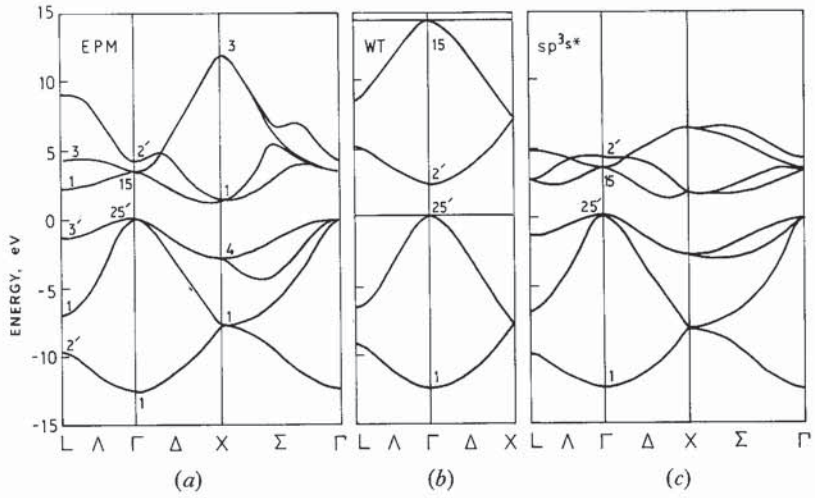

Band structure of c-Si: (*a*) from non-local EPM; (*b*) from the Weaire–Thorpe; and (*c*) from a sp^3s^* first-neighbour hamiltonian.

gap remains. Other forms of disorder must be simulated by varying V_2 and V_1, giving new band limits and an erosion of the gap.

The σ and σ^* states are found whenever well-defined bonds exist. The WT hamiltonian demonstrates that a semiconducting gap remains even when bandwidths are significant [74, 81, 91], a non-trivial problem from the plane wave viewpoint [82, 83]. Although not fully accepted at the time, its conclusions are valid in spite of its oversimplified description of the band structure.

3.3. *The bond orbital model*

The bond orbital model (BOM) [76, 77] is a simplified TB hamiltonian based on that of WT. It can be used to study chemical trends in many properties such as bond energies, ionicities and dielectric constants. The WT hamiltonian is a 8×8 matrix and uses a basis of the sp^3 hybrids $|i\rangle$ and $|j\rangle$ on the two sites. This can be re-expressed in terms of σ and σ^* states, formed from hybrids directed towards each other from each site as:

$$|\sigma\rangle = 1/\sqrt{2}\{|i\rangle + |j\rangle\},$$
$$|\sigma^*\rangle = 1/\sqrt{2}\{|i\rangle - |j\rangle\}. \tag{12}$$

There are two atoms per lattice point in diamond, giving four σ and four σ^* states. Thus it can be re-expressed as 4×4 block matrices

$$H = \begin{vmatrix} \Sigma^* & X \\ X & \Sigma \end{vmatrix} \tag{13}$$

with Σ relating to the σ states, Σ^* to the σ^* states and X coupling the two types. If $V_2 > 2V_1$, the elements of the X block are quite small, and, if neglected, this allows the submatrices for σ and σ^* states to be separated. Many bonding properties may be

studied using only the sub-hamiltonian Σ. Its diagonal elements are the self-energy of the σ states which is V_2 from figure 2. As the σ states are fully occupied the total bonding energy is just the trace of Σ, or $4V_2$. The total energy E_b is the sum of the bonding and promotion energy. The promotion energy, $E(p)-E(s)$, is necessary to convert the ground state s^2p^2 configuration to a sp^3 state [76] and direct evaluation shows that $V_1=\frac{1}{4}\{E(s)-E(p)\}$. Promotion energies are involved in all cases of hybridization. Thus we find

$$E_b=4(V_2-V_1). \tag{14}$$

The BOM also provides a useful model of ionicity and charge transfer [76, 77]. In the zincblende lattice different elements occupy the two sites of the diamond lattice. Their average valence must be four, so this class of compounds is referred to as $\langle 4\rangle$ compounds. The hybrids $|c\rangle$ and $|a\rangle$ on the cation (c) and anion (a) have different self-energies and it is convenient to define its semi-difference as V_3. The hamiltonian of a single bond can be written in terms of $|i\rangle$ and $|j\rangle$ as:

$$H=\begin{vmatrix} -V_3 & V_2 \\ V_2 & V_3 \end{vmatrix} \tag{15}$$

giving σ and σ^* states at energies of V_g and $-V_g$ where

$$V_g^2=V_2^2+V_3^2. \tag{16}$$

The wavefunctions are no longer given by (12) but are now asymmetric

$$|\sigma\rangle=u|c\rangle+v|a\rangle$$

$$|\sigma^*\rangle=v|c\rangle-u|a\rangle. \tag{17}$$

We define the asymmetry of the charge density as the polarity (or ionicity):

$$\alpha_p=u^2-v^2=V_3/V_g. \tag{18}$$

Thus, the asymmetry of σ and σ^* states results from the difference in cation and anion self-energies. The bonding state becomes increasingly anion-like, while the σ^* state is increasingly cation-rich with increasing ionicity and V_3 [77].

In the TB model of very ionic compounds like NaCl, the valence band is constructed of anion orbitals and cation orbitals form the lower conduction bands—in fact the valence band structure can be successfully described by retaining only anion states and anion–anion interactions (which are now second neighbours) [84, 85].

In the original BOM, V_2 and V_3 were parametrized using the optical dielectric constant and certain scaling rules [77, 86]. The model was used to study various aspects of covalence, crystal structure stabilities, optical gaps, effective charges, bond bending force constants, etc. We concentrate on optical excitations. Optical transitions occur by coupling to the electric field, modelled in the BOM by a single dipole matrix element coupling hybrid $|i\rangle$ to $|j\rangle$ along a bond:

$$M=\langle i|x|j\rangle. \tag{19}$$

In the covalent limit, the principle transitions are localized on a single bonding unit, $\sigma\rightarrow\sigma^*$, and produce the E_2 peak. This is broadened by band structure terms like V_1 into the observed spectrum. In the ionic limit the $\sigma\rightarrow\sigma^*$ transitions are now

essentially $|a\rangle \rightarrow |c\rangle$, so the excitation is from anion to cation sites, i.e. a charge transfer [87].

Figure 4 shows that the WT and BOM hamiltonians give a fair representation of the valence bands but a very poor description of the conduction bands. This had led to some questioning of the ability of tight-binding to describe excited states and optical transitions [88–90]. Valence band charge densities are quite localized and are well described by bond orbitals, as can be seen from charge density plots [54, 88]. Most conduction band states are quite delocalized and the antibond orbitals are apparently a poor representation of such states. However, the single bond optical matrix element (19) describes quite well the oscillator strength variations along an isoelectronic series [91]. The second problem is that EPM finds the charge density of the lowest conduction band to become increasingly anion *s*-like with increasing ionicity [88, 89], which appears to contradict the TB notion of ionic conduction bands becoming increasingly cation-like. We note that the σ^* states form four rather than just one conduction bands, and these may have an overall cation character.

It is always possible to describe the valence band of ionic solids with only anion-centred orbitals, but with decreasing ionicity these bear less and less resemblance to pure anion orbitals. The chemical pseudopotential formalism [41, 44] conveniently describes how atomic orbitals are modified when working in a restricted subspace of one band. The practical effect is that the anion orbitals become less atomic in character and more delocalized towards the cations. This effect is sometimes called 'incomplete ionic orbitals' in the language of scattering and resonances [92].

Band structures change in two characteristic ways with increasing atomic number and even the highly simplified WT and BOM models represent these correctly. The most obvious change in the diamond semiconductors is the rapid reduction in average optical gap (E_2), or roughly $2V_2$, from 13 eV in C to 4 eV for α-Sn. The second is the proportionate increase in s–p splittings, $4V_1$. Harrison defined the ratio, $2V_1/V_2$, as metallicity [76]. Increasing metallicity increases bandwidths relative to band gaps and results in an inversion of the Γ_{25} and Γ'_2 states (fig. 4), producing a metallic band structure. This inversion together with the larger promotion energy, $4V_1$, is responsible for the loss of sp^3 bonding in the heavier elements like β-Sn and Pb. Many chemical variations in electronic properties, band structures, co-ordinations or defect properties can be reduced to their dependence on the two basic variables, ionicity and metallicity.

3.4. *The pseudopotential description of covalent bonding*

The nearly-free electron theory of metals requires the electronic kinetic energy (E) to dominate all scattering terms. Thus, for example, the band structure energy $E_{\rm bs}$ of a metal has the perturbative form:

$$E_{\rm bs} = \sum_k V_{\rm p}(k) + \sum_q \frac{V_{\rm p}(q+k)^2}{E(q+k) - E(q)} \tag{20}$$

and provides a successful theory of metal structures [93].

A semiconductor arises in k-space theories when the Jones zone accommodates all the valence electrons and has a forbidden gap over all its faces [94]. The $\langle 220 \rangle$ Bragg planes define the Jones zone of diamond and the large $V_{\rm p}(111)$ pseudopotential produces the gap over the faces. Although numerically smaller, the effect of $V_{\rm p}(111)$ dominates that of the kinetic energy, $E(q)$, over the $\langle 220 \rangle$ faces and cannot

be treated perturbatively [73]. This change in relative importance of V_p and $E(q)$ is disguised in actual EPM calculations as we explicitly diagonalize a matrix of, say, 75 plane waves without considering its detailed composition.

V_p for a binary compound like zincblende is

$$V_p(q) = \sum_{i=1,2} V_i(q) S_i(q) = V_s \cos(q\tau) + iV_a \sin(q\tau), \tag{21}$$

where τ is the bond translation vector along [111] and $V_s = \frac{1}{2}(V_1 + V_2)$ and $V_a = \frac{1}{2}(V_1 - V_2)$ are the symmetric and antisymmetric form factors. On the Jones zone $q\tau = \pi/4$, so V_s and V_a each contribute to the total $V_p(111)$,

$$V_p^2(111) = V_s^2(111) + V_a^2(111). \tag{22}$$

The similarity of eqns. (16) and (22) encourages the identification of V_2 (BOM) with V_s (EPM) and V_3 with V_a. This equivalence is found to hold semiquantitatively [73] and confirms the complementary TB and pseudopotential descriptions of covalence.

The Jones zone of NaCl lattices is also formed from $\langle 220 \rangle$ planes. The centre of symmetry at each atom site changes the structure factor so only $V_a(111)$ contributes to V_p:

$$V_p(111) = V_a(111). \tag{23}$$

Thus, the pseudopotential theory of insulators differentiates ionic from covalent bonding by the centre of symmetry at the ion site [95]. Only antisymmetric potentials contributed to the principal gap.

§4. Parametrizing tight-binding interactions

Tight-binding is capable of producing quite accurate descriptions of the bands, surface and defect states of semiconductors with very simple hamiltonians. Slater and Koster [96] first suggested treating TB interactions as disposable parameters, fitted to other results, with the orbitals themselves remaining spatially undefined. This approach is suitable when the band structure is well established, as for Si, Ge or GaAs [97–100]. The situation is not so fortunate for many interesting amorphous semiconductors, because of their complex crystalline structures (e.g. As_2Se_3). The scaling of interactions with bond length provides a means of transferring TB interactions to these materials [86]. In this section we set down a set of guidelines for estimating TB interactions.

The idea of transferability and scaling grew from experience with EPM factors and from the dielectric theory of bonding in zincblende crystals [51, 101]. The EPM philosophy was to fit the three form factor parameters V_s for each element Si, Ge and Sn to reproduce appropriate experiment data. The V_s were then used unchanged for an isoelectronic series (e.g. Ge, GaAs, ZnSe) because of their equal bond lengths. This leaves only V_a to be fitted empirically for the compounds. For the skew zincblendes with elements from different rows, average values of V_s were used as their bond lengths are derivable from a single set of tetrahedral atomic radii [102]. Scaling first arose in the dielectric theory of bonding [101] when it was found that a symmetric potential, the homopolar gap or E_h, related to $V_s(111)$, depended only on bond length d in a power law fashion:

$$E_h \propto d^{-2.48}. \tag{24}$$

Returning to tight-binding, we first consider the fitting of an established band structure [97–100]. This 'template' is generally a combination of experimental and theoretical results. If available, angle resolved photoemission spectra (ARPES) data are the most reliable for their ability to map out experimentally many of the valence bands and some conduction band features [103–106]. Angle integrated X-ray and ultraviolet photoemission (XPS, UPS) positions the density of states (DOS) features of the valence bands, while band gaps are taken from optical data. Remaining details are then taken from the empirical pseudopotential calculations [54, 88].

Considering Si as an example, we initially use a basis of one s and three p orbitals and retain only first-neighbour interactions [97]. The four first-neighbour interactions $V(ss)$, $V(sp)$, $V(p\sigma)$ and $V(p\pi)$ are conveniently grouped into symmetrical forms, which we label V_{ss}, V_{sx}, V_{xx}, V_{xy}. The hamiltonian is expressed in terms of these terms and the phase factors and is easily diagonalized at Γ, X and L. The parameters are found by equating the band energies at Γ and X to their values in the template, giving bands such as fig. 4(*c*).

TB interactions of C, Si, Ge ad Sn are seen to scale approximately as d^{-2} in fig. 5. Such scaling results from the validity of both EPM and TB at the equilibrium bonding separation, in spite of their opposite free-electron and free-atom viewpoints. The electron kinetic energy scales as d^{-2} forcing a similar behaviour on the TB interactions [86].

Scaling encourages enormous simplifications in TB calculations on complex systems, so its range of validity must be checked [107–109]. The interactions are expressed generally as:

$$V_i = \eta_i d^{-\alpha} \tag{25}$$

with prefactors η_i and a scaling power law α_i. All s, p interactions scale roughly as d^{-2} in sp^3-bonded systems because both s and p orbitals contribute to bonding and the

Fig. 5

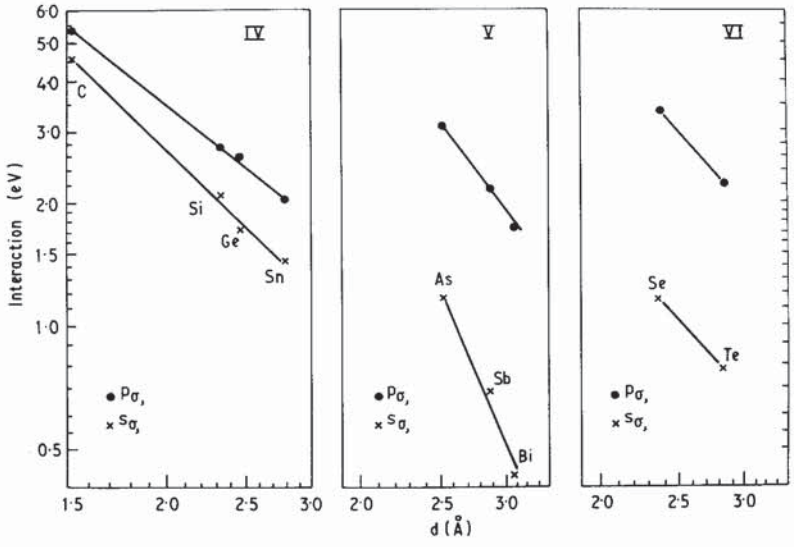

Scaling of tight-binding interactions in group IV and V elements.

observed bond length reflects their combined influence (fig. 5). Group V and VI elements are p bonded. Here, only the $p\sigma$ and $p\pi$ interactions scale roughly as d^{-2}, while the s orbitals are non-bonding and the s interactions decrease more rapidly with d[107, 108] (fig. 5 (*b*)). Another complication is that the prefactors η_i depend on co-ordination number, essentially because overlap effects cause the basis orbitals to differ from pure atomic orbitals in different ways for each co-ordination [86, 108]. Table 1 shows fitted TB parameters for some important elements.

Table 2 gives interactions calculated by the chemical pseudopotential method [6, 110–112], for comparison. Generally, such values have provided a reasonable description of the band structures of sp-bonded solids. Comparing tables 1 and 2, we note that the chemical pseudopotential interactions possess some systematic errors: they tend to underestimate $V(pp\sigma)$ and thereby optical gaps, they also do not contain any dependence on co-ordination number, unless the true local orbitals rather than atomic orbitals are used.

The TB parametrization of compounds is a generalization of the method for elements and can be summarized thus:

(1) The two-centre interactions are analogous to V_s in EPM, depend only on bond length and not charge transfer, so scaling is valid [5, 109].
(2) The orbital energies are close to their free atom energies [109].

This latter result may be somewhat surprising as charge transfer produces sizeable Madelung energies. However, their effects are balanced by equal intra-atomic shifts

Table 1. Tight-binding parameters (in electronvolts) found by fitting established band structures. C to Sn in the diamond structure, C as graphite, As-Bi in the A7 structure and Se, Te in the trigonal structure. The zero of energy is the valence band maximum or the Fermi level in graphite.

	d (Å)	$V(ss)$	$V(sp)$	$V(p\sigma)$	$V(p\pi)$	$V(s^*p)$	$E(s)$	$E(p)$	$E(s^*)$
C	1·55	−4·54	5·15	5·30	−1·52	3·55	−2·85	3·0	17·0
Si	2·35	−2·08	2·48	2·72	−0·72	2·32	−4·2	1·72	6·73
Ge	2·45	−1·70	2·36	2·56	−0·67	2·26	−5·88	1·61	6·39
Sn	2·81	−1·42	1·95	2·18	−0·60	1·81	−5·67	1·33	5·90
	d, (Å)	$V(ss)$	$V(sp)$	$V(p\sigma)$	$V(\pi_{xx})$	$V(\pi_{zz})$	$E(s)$	$E(p)$	
graphite	1·42	−5·18	5·34	5·79	−1·72	−2·92	−3·75	0·48	
	d, (Å)	$-V(ss)$	$V(sp)$	$V(p\sigma)$	$V(p\pi)$		$E(s)$	$E(p\sigma)$	$E(p\pi)$
As	2·51	−1·17	1·60	3·10	−0·79		−11·0	−1·0	
	3·15	−0·53	0·80	1·66	−0·29				
Sb	3·90	−0·67	1·14	2·17	−0·51		−9·0	−0·4	
	3·37	−0·33	0·50	1·25	−0·14				
Bi	3·10	−0·43	0·78	1·75	−0·32		−10·2	−0·4	
	3·47	−0·23	0·36	1·09	−0·08				
S	2·03	−2·6	3·0	4·9	−1·2		−14·4	−1·6	−1·6
Se	2·37	−1·11	2·10	3·37	−0·92		−12·4	−1·06	−1·92
	3·44	−0·22	0·20	0·64	−0·10				
Te	2·83	−0·78	1·60	2·10	−0·78		−10·1	−1·45	−1·55
	3·50	−0·23	0·15	0·70	−0·04				

Table 2. Tight-binding interactions (in electronvolts) found by the chemical pseudopotential method [112]. A larger potential is used then in [111], see page 185 of [6].

	d (Å)	$V(ss)$	$V(sp)$	$V(p\sigma)$	$V(p\pi)$
Si	2·35	−1·77	2·54	2·48	−0·93
Ge	2·45	−1·76	2·47	2·30	−0·81
P	2·23	−1·74	2·61	2·73	−0·99
	3·17	−0·34	0·71	1·08	−0·27
As	2·51	−1·42	2·11	2·41	−0·83
	3·15	−0·40	0·78	1·23	−0·29
Sb	2·91	−0·90	1·51	1·81	−0·59
	3·38	−0·44	0·87	1·19	−0·33
Se	2·37	−1·65	2·70	2·97	−0·93
	3·44	−0·18	0·46	0·76	−0·17
Te	2·83	−0·90	1·51	1·81	−0·59
	3·50	−0·44	0·87	1·18	−0·33

in orbital energies due to the changing orbital occupations [109]. Thus, free atom orbital energies may be used for most sp-bonded solids, even NaCl [5]. There are three cases where inadequate screening requires self-consistency to be included explicitly in TB: molecules [113], d orbitals [114] and certain co-ordination defects [115].

More distant interactions must be included in the ionic compounds. The last section noted how their valence and conduction bands tend to be formed from orbitals localized on the anions and cations, respectively. Thus the effects of second-neighbour like-atom interactions begin to dominate the nearest-neighbour unlike-atom interactions. If only a valence band is desired, one can even retain only anion-like orbitals and use only (renormalized, i.e. larger anion–anion interactions. If both valence and conduction bands are desired interactions between both like and unlike species must be included. The first-neighbour interactions are similar to those in zincblende, and second-neighbour interactions are close to those given by the chemical pseudopotential method or can be exponentially scaled from first-neighbour interactions [109]. Tight-binding parameters for selected heteropolar systems are given in tables 3–7, found by fitting to other calculations and experiments.

Table 3. Tight-binding interactions (in electronvolts) for GaAs using sp^3s^* basis [99]. (c = cation (Ga); a = anion (As)).

	$V(ss)$	$V(sc,pa)$	$V(sa,pc)$	$V(p\sigma)$	$V(p\pi)$	$V(s^*c,pa)$	$V(s^*a,pc)$
GaAs	−1·61	2·50	1·93	3·03	−0·78	2·08	2·10

	$E(s)$	$E(p)$	$E(s^*)$
Ga	−2·66	3·66	6·74
As	−8·34	1·04	8·59

Table 4. Tight-binding interactions (in electronvolts) for SiO_2 using sp^3 basis and including second-neighbour O–O interactions (c=Si, a=O).

SiO_2	$V(ss)$	$V(sc,pa)$	$V(sa,pc)$	$V(p\sigma)$	$V(p\pi)$
Si–O	−3·0	5·4	5·0	6·0	−1·4
O–O				0·56	−0·13

	$E(s)$	$E(p)$
Si	5·1	11·1
O	−1·08	−16·0

Table 5. Tight-binding interactions for Cs_3Sb of both first and second neighbours [264].

Cs_3Sb	d (Å)	$V(ss)$	$V(sc,pa)$	$V(sa,pc)$	$V(p\sigma)$	$V(p\pi)$
Cs–Sb	3·95	−0·36	0·85	−0·58	0·81	0
Cs–Cs	3·95	−0·24	0·53		0·70	0
Cs–Sb	4·56	−0·24	0·62	0·22	0·64	−0·13
Cs–Cs	4·56	−0·24	0·38		0·64	−0·13

	$E(s)$	$E(p)$
Cs	−3·60	−1·60
Sb	−14·82	−7·26

Table 6. Tight-binding interactions (in electronvolts) for CsAu, using Cs sd^2, Au sp^3 basis, used for fig. 36.

CsAu	$V(ss)$	$V(sp)$	$V(p\sigma)$	$V(p\pi)$	$V(sd)$	$V(pd\pi)$	$V(dd\sigma)$
Cs–Au	−0·19	0·53	—	—	−0·02	0·7	
Cs–Cs							−0·6
Au–Au	−0·21	0·22	0·6	0·25			

	$E(s)$	$E(p)$	$E(d)$
Cs	9·9	—	7·8
Au	−1·26	5·5	—

Table 7. Tight-binding interactions for the Si–H bond. (*a*) After Pandey [533], including only the H *s* orbital. (*b*) After Robertson [532], including H sp^* orbitals and only Si–H interactions. The energy zero is the band edge of bulk c-Si.

	$V(ss)$	$V(sp)$	$V(p,p^*)$	$E(H,s)$	$E(H,p^*)$	$E(\mathrm{Si},s)$	$E(\mathrm{Si},p)$
(*a*)	−3·57	2·76		−3·38	—	−4·20	0·19
(*b*)	−3·52	3·22	2·46	−3·38	6·73	−4·20	1·72

Descriptions of the covalent solids are often improved by including higher order interactions or adding excited orbitals to the simple sp^3 basis. A number of general observations can be made. The first-neighbour interactions usually change when higher order interactions are included, as parameters depend on truncation, whether in TB or EPM. Secondly, the overlap of intervening atoms cause the interactions between distant neighbours to differ from the direct interaction. Excited orbitals have been used recently to improve the conduction of zincblende [99], PbTe-like [107] and Mg_2Si-like semiconductors [116]. This required only minor additions and improves an often criticized feature of TB bands.

This section can be summarized in a set of guidelines for TB calculations on arbitrary non-crystalline systems. Firstly, a random or periodic structure must be chosen which simulates the desired SRO. The bond lengths should be taken from atomic radii if not known experimentally. If the system has a thoroughly studied crystalline analogue, one should fit this band structure and use these parameters, after minor scaling if bond lengths differ. Otherwise, it is necessary to choose a reference system for each bond type with a similar co-ordination and electron density from which to scale to interactions. The prefactors η_i depend on co-ordination and the scaling power α_i depends on valence. These are selected by

Table 8. Hartree–Fock energies (in electronvolts), tetrahedral and 8-N covalent radii (in Ångstroms) of main-group atoms. For some first row elements the atomic radius of bonds to Si are much smaller, and also shown (from SiH_4, Si_3B_4, β-Si_3N_4, c-SiO_2 and SiF_4).

	Li	(H)	Be	B	C	N	O	F
$-E(s)$	5·34		8·41	13·46	19·37	26·62	34·02	42·78
$-E(p)$				8·43	11·07	13·84	16·72	19·86
$r\langle 4\rangle$			0·98	0·85	0·77	0·72	0·68	0·67
$r\langle 8\text{-}N\rangle$					0·77	0·75	0·74	0·71
$r\langle \mathrm{Si}-X\rangle$		0·31		0·89		0·55	0·44	0·42
	Na		Mg	Al	Si	P	S	Cl
$-E(s)$	4·95		6·88	10·70	14·79	19·22	24·01	29·2
$-E(p)$				5·71	7·58	9·54	11·60	13·8
$r\langle 4\rangle$			1·30	1·23	1·17	1·13	1·13	1·13
$r\langle 8\text{-}N\rangle$					1·17	1·10	1·03	0·99
	K	Ca	Zn	Ga	Ge	As	Se	Br
$-E(s)$	4·01	5·32	7·96	11·55	15·15	18·91	22·86	27·0
$-E(p)$				5·67	7·33	8·98	10·68	12·43
$r\langle 4\rangle$			1·23	1·23	1·23	1·23	1·23	1·23
$r\langle 8\text{-}N\rangle$				1·26	1·23	1·25	1·17	1·14
	Rb	Sr	Cd	In	Sn	Sb	Te	I
$-E(s)$	3·75	4·85	7·21	10·14	13·04	16·02	19·12	22·34
$-E(p)$				5·37	6·76	8·14	9·54	10·97
$r\langle 4\rangle$			1·41	1·41	1·41	1·41	1·41	1·41
$r\langle 8\text{-}N\rangle$					1·41	1·43	1·34	1·33

reference to fig. 5. Second-neighbour interactions should only be included for ionic phases or if explicit fitting shows them to be necessary. The free atom energies are used initially for the orbital energies. At a second stage, the orbital energies should be varied to fit optical gaps and other interactions modified to fit any photoemission data available for the system concerned. For convenience, the orbital energies of free atoms are listed in table 8, together with atom radii. Two types of radii are included for different co-ordinations, firstly for '8-N' co-ordinations, and also tetrahedral radii.

§ 5. Electronic structure of the elements

5.1. *a-Si and a-Ge*

a-Si and a-Ge are the best understood of the $\langle 4 \rangle$ elements while a-C is complicated by the presence of competing three-fold and four-fold sites and a-Sn is virtually unstudied. The SRO and rdf of c-Ge was discussed in § 2.1 (fig. 1) and is similar to that of a-Si. Each Ge site is approximately tetrahedral, with essentially no bond length distortion and a $\pm 9\%$ angle disorder. The dihedral angle distribution favours *trans* over *cis* angles by about 2 : 1 in the most accurate study [30]. Our best knowledge of ring statistics comes from analysis of the s band DOS, discussed shortly, a-Si : H is distinct from a-Si and is considered in § 8.6.

The electronic structure of a-Si and a-Ge can be described by TB hamiltonians by varying complexity, the appropriate one depending on the application [73–77, 97–100, 117–119]. Their parameters should be calibrated against the non-local EPM bands of c-Si and c-Ge [54, 88]. The origin of the gap and the s-band DOS can be studied using the WT and BOM hamiltonians [73–77]. These hamiltonians are based on sp^3 hybrids and retain only the intra-atomic and intrabond interactions, V_1 and V_2 (fig. 2). Their valence bands are very simple, with two flat upper bands due to the absence of π interactions and their conduction bands are very poor. The inclusion of all first-neighbour interactions gives generally good valence bands [97]. Their remaining error is the absence of dispersion along XW, needed to increase the width of the upper p bands, as seen in photoemission. This requires the inclusion of second-neighbour interactions [97]. The simplest hamiltonians all fail to reproduce the indirect gap of the lowest conduction band. This requires additional interactions such as in the second-neighbour scheme of Pandey and Phillips [117]. States deep in the band gap such as dangling bonds possess both valence and conduction band character, and can only be correctly modelled by hamiltonians which reproduce both bands with similar accuracy [118]. The description of such deep states and of the conduction band is becoming of increasing intereest. The Pandey–Phillips [117] parameters produce too narrow conduction bands for this purpose but other second- or third-neighbour schemes are successful [118, 119]. Perhaps the most efficient hamiltonian for defect states is due to Vogl *et al.* [99]. It has only first-neighbour interactions but an extended sp^3s^* basis. The interaction $V(s^*p)$ produces the indirect gap, and it gives better defect states than many more complex schemes. TB parameters within this scheme are given in table 1 for C, Si, Ge and Sn.

Figure 6 shows the XPS spectra of c-Si and a-Si [120]. We divide the DOS into four regions, the lower s valence bands, the valence p bands, the pseudogap and the conduction band. The most noticeable changes in the valence band are the merging of the twin peaks of the s-band of c-Si into a single peak in a-Si and the steepening of

Fig. 6

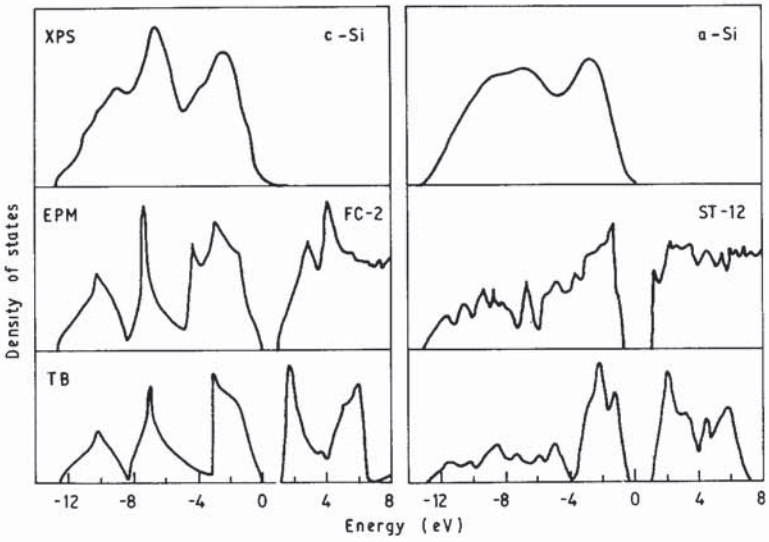

(*a*) Density of states of c-Si from XPS, EPM and from the sp^3s^* TB hamiltonian. (*b*) DOS of a-Si from XPS [120], compared with calculated DOS from EPM [67] and sp^3s^* TB on ST-12 aligned to the valence band edge of the TB calculation [126].

the upper edge of the p peak. The merging of the s peaks is due to the presence of odd-membered rings of bonds, originally shown by the WT model [74]. The simplest explanation considers s orbitals at the sites of isolated rings of bonds. Their eigenvalues are at:

$$\varepsilon = 2S\cos\frac{2\pi n}{N}, \qquad n = 1, 2, \ldots, N, \tag{26}$$

where S is the interaction and N the ring order. The diamond or FC-2 lattice possesses only six-membered rings whose eigenvalues avoid $\varepsilon = 0$. In contrast, the states of five- and seven-fold rings lie close to $\varepsilon = 0$ and they fill in the dip of the s band. This argument is confirmed by EPM calculations on Si polymorphs [67] and by recursion calculations on two random networks, that due to Polk [31] and the Connell–Temkin model [33] which contains only even rings and whose s band DOS retains the dip [121]. The polymorphs show a similar effect; of the polymorphs FC-2, 2H-4 (wurtzite), BC-8 and ST-12, only ST-12 contains odd-rings [122, 123] (five-fold in this case) and it has a broad s band DOS [70, 124–126].

The sharpening of the p band has been studied using polymorphs, Bethe lattices and analytic means [67, 70, 124–127]. In increasing complexity the FC-2 polymorph contains only six-fold rings of *trans* bonds, and 2H-4 only six-fold rings, a third of whose bonds are now *cis*. BC-8 possesses bond angle disorder while ST-12 has two types of site, large bond angle disorder and five-fold rings. Joannopoulos [67, 70] originally attributed the sharpening of the p band to bond angle disorder from his EPM polymorph calculations and his later Bethe lattice results. In contrast, Singh

[127] attributed the sharpening to *cis* bonds and dihedral angle disorder. The author [126] supports the latter conclusions following TB calculations on the polymorphs using the sp^3s^* hamiltonian shown in fig. 6. Now, while EPM is more accurate than TB, TB has the advantage that the orbital energies act as a reference energy which allows us to attribute changes in the gap to either a movement of the valence or conduction band edge. The gap of FC-2 Si is 1·1 eV. In EPM 2H-4 was found to have a similar gap (0·85 eV), BC-8 a very reduced gap (0·43 eV) and ST-12 a large gap (1·6 eV). In TB, the gap of FC-2 is 0 to 1·1 eV, in 2H-4 0 to 1·3 eV, BC-8 0·4 to 0·9 eV and ST-12 −0·6 to 0·9 eV, emphasizing that the valence band retreats in ST-12 but not 2H-4. Thus, fig. 6 shows the EPM DOS for FC-2 and ST-12 aligned using the band edges from the TB calculations and the retreat of the valence edge of ST-12. The importance of dihedral angle effects can be easily overlooked using polymorphs if 2H-4 is used as the prime example because its limited form of dihedral disorder does not shift the valence maximum. In contrast, the five-fold rings of ST-12 necessarily contain *cis* bonds so ST-12 also possesses strong dihedral disorder, confirming that such disorder is the source of the sharpening.

The WT hamiltonian predicts a higher conduction band minimum a-Si because of the absence of pure σ^*s states [81]. The phase of such states must alternate across a bond so they cannot exist around odd-numbered rings—an example of a frustrated plaquette. The absence of such states in a-Si could limit the conduction bandwidth. However, both c-Si and c-Ge have indirect gaps and in Si the σ^*s Γ_2' state actually lies at 4·3 eV, so the absence of such states has little practical effect on the gap in a-Si [126]. Thus the conduction band edge is little affected by disorder theoretically, which photoemission confirms [4].

In contrast to the valence band, the conduction band DOS is relatively featureless. The experimental $L_{2,3}$ ($2p$) core spectrum of c-Si and a-Si is compared in fig. 7 [128]. This spectrum measures the partial s densities of states, which is seen to be much flatter in a-Si. The calculated conduction band DOS of ST-12 is also found to be flat, showing that the variety of dihedral angles and rings of bonds to be responsible for the change [67]. The core spectra possesses a sharper leading edge in a-Si than c-Si (fig. 7). This feature is attributed to a core exciton which becomes slightly more tightly bound in a-Si. The $Z+1$ approximation [129] models the core excited atom as a substitutional donor (phosphorous for Si) and TB calculations suggest that substitutional P states are slightly deeper in a-Si than c-Si, so the exciton is deeper in a-Si [126]. The K ($1s$) absorption spectrum measures the partial p conduction band DOS. It also has a steeper edge in a-Si than c-Si [130]. However, the larger Auger width of the $1s$ level results in a poorer resolution.

The optical spectra of a-Ge and a-Si are distinctively different from those of the crystals [131, 132]. The latter are sharply peaked, c-Si at 4·4 eV and c-Ge at 4·3 eV, while the amorphous spectra are broad peaks, displaced towards lower energies (fig. 8). The changes are due partly to the lack of a k selection rule [1, 132]. This rule delays transitions in indirect gap crystals till higher energies, while in amorphous semiconductors valence states can be excited to all conduction states. In fact, if the energy dependence of the matrix elements is taken to be that of c-Ge and a flat conduction DOS is assumed, the experimental ε_2 spectra of a-Ge can be deconvolved to give a very realistic valence DOS [131]. Again, studies with polymorphs [68, 126] have shown that the distribution of dihedral angles and ring statistics smooths out the ε_2 spectra (fig. 10 (*b*)). A similar analysis could be performed using Bethe lattices [133].

Fig. 7

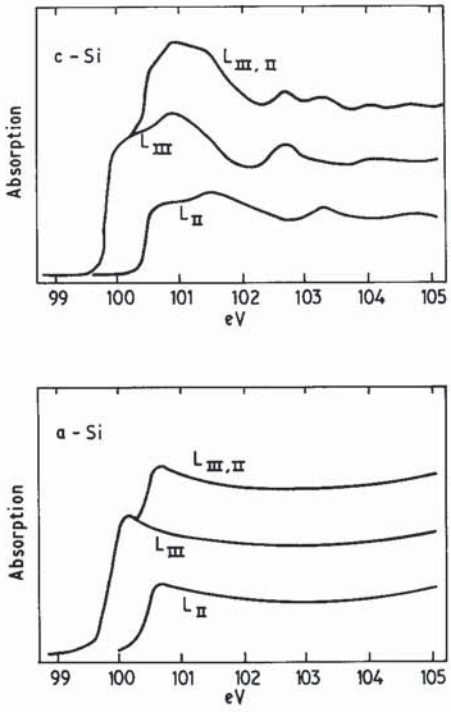

Core absorption of the Si $L_{2,3}$ edge in c-Si and a-Si, showing the sharpened edge and flattened conduction band DOS of a-Si.

Fig. 8

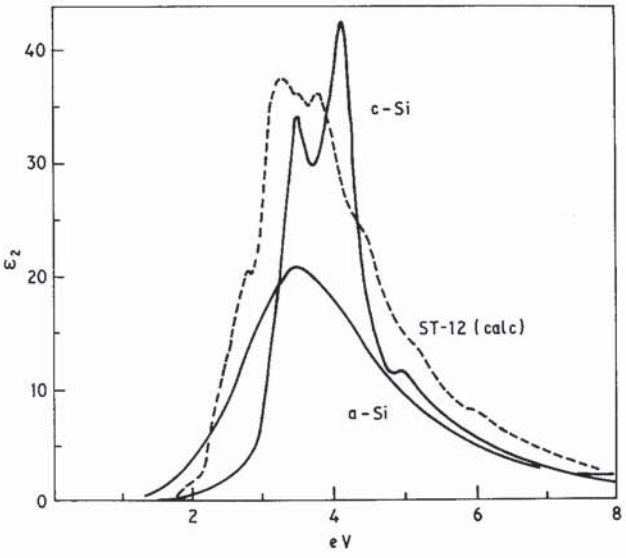

Experimental optical ε_2 for c-Si, and a-Si [132], compared to the ε_2 of ST-12 Si calculated by EPM [68].

5.2. *a-C*

a-C is atypical of the group IV elements because its SRO is largely graphitic rather than diamond-like. Graphite is a layered lattice with strong sp^2 intralayer bonding and very weak interlayer interactions. The mirror plane of each layer separates its bands (fig. 9 (*a*)) into even σ states formed from the sp^2 hybrids and the odd π states around ε_f which cause its semimetallic character [134–137, 108]. Diamond is an isotropically sp^3-bonded insulator with a 5·5 eV band gap with a band structure similar to that of Si (fig. 9 (*b*)) [105, 138–140].

a-C can be prepared by a variety of techniques, such as electron-beam evaporation, sputtering or the glow discharge decomposition of hydrides like C_2H_4 [141–148]. Its properties depend on the deposition temperature even more strongly than those of a-Si and the hydrogen content of the GD films, of order 35%, is also much greater [146].

The key structural issues for a-C are the relative importance of three- and four-fold sites and the extent to which the large H content saturates graphitic bonding in a-C : H. The extreme hardness and semiconducting nature of a-C was early evidence for sp^3 bonding, but the Raman spectra show that graphitic bonding is overwhelming [147]. The electron energy loss and XPS spectra of a-C are very similar to those of graphite [141] (fig. 10). A model of a-C of graphitic islands of about 20 Å diamond has been proposed to interpret the data for a-C [147]. There is, however, the problem of the origin of the semiconducting gap of 0·5 eV in a-C [143] and of 1·5–2 eV in a-C : H [146]. A pseudogap can be created by localizing existing states if their density is sufficiently low [1]. The DOS of crystalline graphite does possess a sharp minimum at ε_f [136] but its width depends strongly on interlayer interactions and is only a small fraction of the total π bandwidth. Thus, to produce a gap, the structural

Fig. 9

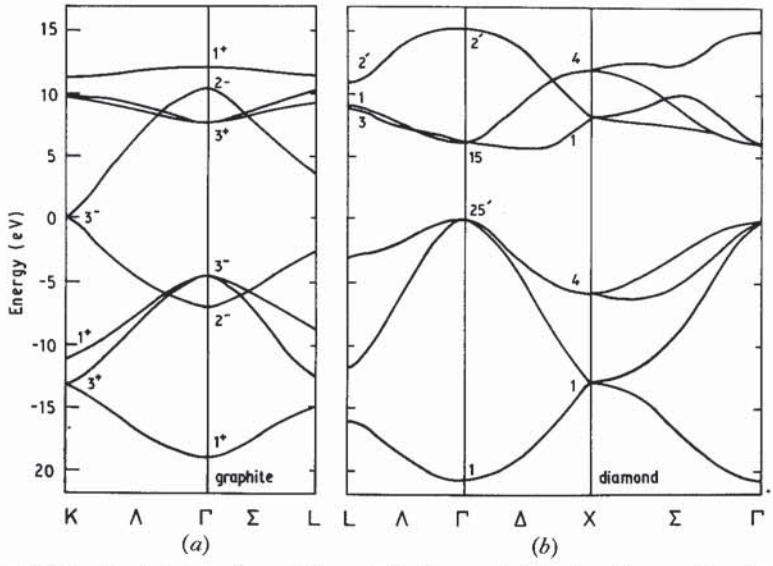

TB bands of (*a*) a single layer of graphite and (*b*) diamond. The bands were fitted to APRES [105, 137] and previous calculations [134, 138].

Fig. 10

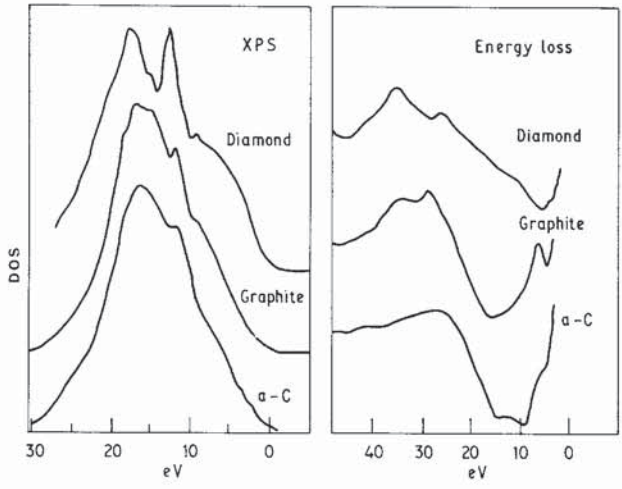

XPS and energy loss spectra of diamond, graphite and a-C (after [141]).

disorder must be of the type that localizes these states rather than causes further tailing into the gap. We note that an ESR signal corresponding to about 3×10^{19} spins/cm^3 is observed and is usually attributed to dangling bonds [147]. This density is three orders of magnitude less than the number of broken bonds at the edges of 20 Å islands so reconstruction must occur, perhaps producing tetrahedral sites.

We propose a more definite structural model in which graphitic islands interconnect via four-fold sites, leaving few dangling bonds. TB calculations on an idealized tetragonal simulation of such a structure were carried out. The DOS shows a well-defined gap of 2 eV for a periodicity of two hexagonal rings between the tetrahedral sites and decreases to 1 eV for a periodicity of 12 rings, equivalent to 20 Å islands [149]. The four-fold sites correcting the islands do not possess π orbitals, thereby quantizing the π band of intervening sites and producing the semiconducting π–π^* gap.

Energy loss, photoemission and vibrational spectra of a-C : H would be valuable as they would show the extent of saturation of the graphitic bonding by hydrogenation.

5.3. *a-P, a-As, a-Sb and a-Bi*

The amorphous pnictides or group V elements are often noted to have properties intermediate between the tetrahedrally bonded group IV elements and the divalent chalcogens [38]. In terms of electronic structure, the group V and VI elements are more closely related, as both are p bonded and have a split first co-ordination shell of covalently bonded neighbours and weaker back-bonded neighbours. Considering other properties, no group IV element forms a glass, while As, Se and S all do. However, the presence of midgap states in a-As allows variable-range hopping near ε_f under pressure [38], as in Ge but not Se. The most important similarity between pnictides and chalcogens is that the bonding in their amorphous phases becomes